A Photographic Study of the Neutron Spectra from Al(αn) and Si(dn)*

R. A. Peck, Jr.
Sloane Physics Laboratory, Yale University,† New Haven, Connecticut

(Received January 15, 1948)

The two neutron spectra named have been studied by the photographic method, using the new Eastman NTB nuclear particle emulsion. Details of the experimental method are discussed, with reference also to some features of the histogram representation employed here. The following mass differences are obtained:

$$P^{30}-Al^{27}=2.998\ 06\pm0.24\times10^{-3}\text{ mass units},$$
$$P^{29}-Si^{28}=1.006\ 64\pm0.14\times10^{-3},$$
$$P^{30}-Si^{29}=1.002\ 15\pm0.21\times10^{-3},$$
$$P^{31}-Si^{30}=1.000\ 88\pm0.18\times10^{-3}.$$

A level in P^{30} at 1.02 ± 0.12 Mev above ground is found and confirmed, and three levels in P^{31} established. Group widths and intensities are listed.

1. INTRODUCTION

SINCE a given atomic nucleus may be formed as the end product of any of several cyclotron-induced reactions, the study with a single bombarding instrument of such series of reactions may be expected to yield internally consistent mass values for, and possibly selection rules in the formation of, the several product nuclei involved. This paper deals with four neutron-yielding reactions studied by the photographic-microscopic method of observation of recoil hydrogen nuclei originating within the photographic emulsion. These protons, elastically scattered by the incident neutrons, produce columnar ionization and, consequently, microscopically observable tracks in the emulsion, which thus assumes the character of an extremely large, continuously sensitive, hydrogenous cloud chamber. Measurements on the range distribution of the recoil protons allow the determinations of their energy distribution and, in turn, the energy distribution of the neutrons impinging on the emulsion. A comprehensive examination of the present characteristics of photographic detection has recently been given by Lattes, Fowler, and Cuer.[1]

The reactions here studied are:

$$Al^{27}+He^4=P^{30}+n^1+Q_1, \quad (1)$$
$$Si^{28}+D^2=P^{29}+n^1+Q_2, \quad (2)$$
$$Si^{29}+D^2=P^{30}+n^1+Q_3, \quad (3)$$
$$Si^{30}+D^2=P^{31}+n^1+Q_4. \quad (4)$$

Neutrons from (1) have been observed by several investigators, though no complete energy spectrum appears to have been published. However, the excitation curve for the reaction has been obtained by Waring and Chang,[2] Pollard, Schultz, and Brubaker,[3] and Fünfer;[4] the favored value for the threshold excitation seems to be approximately 2.0 ± 0.2 cm for the alpha-particle range. No data were found in the literature pertaining to reactions (2) to (4), other than the predicted[5] Q-values, $+3.9$ and $+4.3$ Mev for (3) and (4), respectively.

2. EXPERIMENTAL DETAILS

Exposure

Bombarding particles were in all cases accelerated in the cyclotron, which provided approximately 0.03 microampere of 7.6-Mev alpha-particles or 1 microampere of 3.7-Mev deuterons.

* Part of a dissertation presented to the Faculty of the Graduate School of Yale University in candidacy for the degree of Doctor of Philosophy.

† Assisted by the O.N.R. under Contract No. N6ori-44.

[1] C. M. G. Lattes, P. H. Fowler, and P. Cuer, Proc. Phys. Soc. London 59, 883 (1947).

[2] J. R. S. Waring and W. Y. Chang, Proc. Roy. Soc. 157, 652 (1936).

[3] E. C. Pollard, H. L. Schultz, and G. Brubaker, Phys. Rev. 53, 351 (1938).

[4] E. Fünfer, Ann. d. Physik 32, 313 (1938).

[5] M. S. Livingston and H. A. Bethe, Rev. Mod. Phys. 9, 245 (1937).

An ultimate limit on the practicable exposure of photographic plates is set by the gamma-ray background from the cyclotron chamber. That limit is reached when the random grains, which develop in the emulsion in response to the background gamma-rays, are so frequent as to render uncertain the identification of the beginning of a proton track. The limiting exposure is considerably increased by the use of thick lead shielding for the plates. The arrangement used provided a minimum of 10 cm of lead on all sides, except in the direct path of neutrons from the target.

The plates were held in a small box made of lead to minimize protons knocked on from the holder material. They were arranged to intercept neutrons emitted at 90° (in the laboratory system) to the direction of projectile incidence, and, with their emulsions in the horizontal plane, subtended angles not greater than $\pm 3°$ about the 90° position. This fore-and-aft spread can be completely eliminated by rotating the plates into a vertical plane.

The effect of collimation of neutrons from the target is achieved by keeping the plates at least a certain distance from the target. The same solid angle limitation which thus affords collimation also reduces yield, effecting an upper limitation on the plate-to-target separation. In the present work all plates were kept between 18 and 19 cm from the bombarded sample, providing adequate yield and good geometry.[6]

Photography

The new Eastman NTB emulsions were used, batch number 347,126, coated on 1×3 inch microscope slides. The emulsion contained 85 percent AgBr by weight and was 51 ± 7 microns thick when exposed, shrinking to 20–25 microns when processed. The batch was calibrated with a standard group of protons at successively reduced values of energy.[7] Since appreciable fading of the image was noted when development was delayed two days after exposure, it has been the practice to process plates within a few hours of their use.

Satisfactory tracks were obtained by developing for 3 to 4 minutes in Eastman D8. Development was followed by a 2 minute rinse in the stopping solution SB 1-a, and fixing in acid hardening solution F5. All processing was done at room temperature, the normal variation in which did not appear to alter the track quality appreciably. The plates were then washed in a slow current for approximately 30 minutes, and allowed to dry (emulsion up) on blotting paper, covered with an inverted glass dish. The dried emulsions were covered with No. 0 microscope slide cover glasses, using as adhesive a suspension in xylene of the resin damar. In addition to protecting the emulsion surface, this procedure has the advantages that (a) dust particles floating in the gum aid in locating (microscopically) the emulsion surface, and (b) mechanical scratches in the surface are filled in and largely rendered invisible by the damar suspension.

Microscopy

A Bausch & Lomb binocular microscope (Model CT) fitted with a mechanical stage was used. Verniers on the stage, with least count 0.1 mm, allowed easy resetting on a track at low magnification. Two pairs of eyepieces, compensated for use with apochromatic objectives and having magnifications 10× and 25×, were used with the following objectives: apochromat, 10×, 16 mm, 0.30 NA, dry; apochromat, 20×, 8.3 mm, 0.65 NA, dry; apochromat, 90×, 2 mm, 1.30 NA, oil; achromat, 45×, 4 mm, 0.85 NA, dry, with iris diaphragm.

When the limited abundance of tracks necessitated searching the plates at the lowest available magnification (100× over-all), a system of oblique illumination was used. True dark field illumination was not obtainable at this magnification, though quasi-dark field was advantageous, to minimize eyestrain. One of the first conditions to be applied in selecting tracks for close scrutiny is that all acceptable ones must be traveling in approximately the same direction. But the oblique system illuminates preferentially tracks having a particular orientation and, consequently, effects automatically a rough preselection of tracks with respect to direction. In effect, scanning is made easier with oblique illumination by the apparent elimination of irrelevant, off-angle tracks. Measurements were, in the main, made at 450× magnification. A

[6] Reference 5. Here, a/b was approximately 0.05 in all cases, while $\cos\theta_0$ ranged from 0.1 to 0.4.

[7] R. A. Peck, Jr., Phys. Rev. **72**, 1121(L) (1947).

considerable advantage was gained from an iris in the high dry objective. This allowed a variability in focal depth with the 450× system, so that track measurements were made with ease and at the same time many tracks could definitely be established as originating and terminating within the emulsion by observing grains in focus above and below the ends. For those tracks requiring an even shallower focus for the latter discrimination, the immersion objective (900× over-all) was used. An alternative system which has been found convenient in the case of somewhat higher yields employs the 25× eyepieces, scanning at 250× over-all with oblique illumination, measuring and discriminating at 1125× (high dry), at which excellent dark field is obtainable.

In addition to the obvious necessity that a track begin and end within the emulsion, an acceptable track was required to lie within the square cone $\pm 11°$ about the direction of neutron incidence, in both the plane of the emulsion and that normal to it. Two criteria thus appear, with separate techniques for their application. The horizontal angle test is easily applied, for any angle in the emulsion plane can be pre-set by the use of a diametrical hairline in each of the paired oculars. The maximum allowable angular divergence in the vertical plane is related, in terms of the focal depth of the system, to a minimum length of track which is required to be in focus at a single setting. The vertical criterion applies to the emulsion when exposed, and must be corrected in application for the shrinkage of the emulsion which occurs during processing.

This pair of criteria effectively selects for measurement those tracks moving in a particular direction, that of the incident neutrons. A considerable simplification in the handling of data derives from the consequence that all tracks measured correspond directly to neutron energies, unreduced.[8]

Track measurements were accomplished by the use of an eyepiece scale, calibrated by reference to a stage micrometer. When track scattering occurred, a conventional[1] procedure was adopted. Direction changes in the plane of the emulsion were followed by re-orienting the eyepiece scale, while changes in the angle of dip (in the plane normal to the emulsion) were ignored, unless they took the track at any point outside of the maximum obliquity acceptable in that plane. The small inaccuracies thus introduced into some length measurements is the price of the considerable increase in operational facility.

3. TREATMENT OF THE DATA

Each set of data is represented graphically in the form of a histogram, in which are plotted successive values of the number of tracks with length between certain values. The numbers of tracks are plotted as a function of some length characteristic of the interval used, and the interval is moved uniformly along the scale of range or energy. It seems proper that the constant interval of the histogram should be constant in terms of energy rather than range. On the other hand, the use of extrapolated range as a defining property necessitates plotting on a linear range (not energy) scale, which indeed is the most convenient procedure. Therefore, the histogram interval used has been made to increase with range in such a manner as to preserve the magnitude of the equivalent interval in energy. This is easily accomplished in a calibrated emulsion, for the air range-energy curve[5] and the stopping power-energy function[7] render equivalent the quantities emulsion range, air range, and energy. As abscissae in the histograms, the median value of the tracks in each interval has been used so long as the number of those tracks remained high. When the number of those tracks dropped below 10 (arbitrary), the median was replaced by the mean length of the tracks involved. This procedure has the advantage of giving some indication of the distribution of tracks within the interval, but the disadvantage that low yield regions of short extent tend to appear as depopulated areas on the graph, rather than areas with small ordinates typically spaced. The prime advantage to the use of the median, of course, is the time saved in plotting.

For the fuller expression of the significance of each set of data, the histograms plotted have been of an "overlapping" type. For example, the spectra in this paper represent tracks per

[8] H. T. Richards, Phys. Rev. 59, 796 (1941).

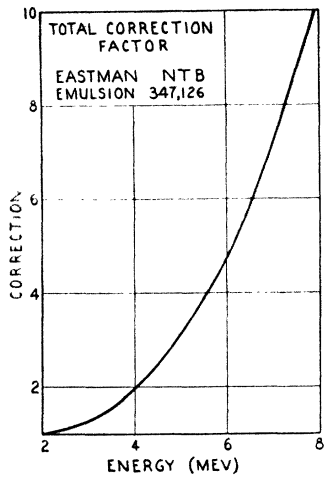

FIG. 1. Product of geometrical and cross-section correction functions for Eastman NTB emulsion 347,126. Thickness 51 microns.

200-kev interval calculated and plotted every 100 kev. Each datum, in general, is thus represented twice on the graph, and the area beneath the curve corresponds approximately to twice the number of tracks observed.

A strong observer bias has been noted in the recording of the last significant (estimated) figure of range values. This bias offers an absolute limit to the significant resolution possible with a given eyepiece scale and optical system. It is further to be expected that the bias may lead to spurious structure in a given histogram, revealed as a falsely high or low yield at a particular locus due to the accidental location of a boundary between successive intervals. This structure was partly rejected by the use of overlapping histograms as just described, and also by plotting, on the same graph, two or more point sets representing histograms with their starting points shifted by arbitrary amounts. Whatever characteristics survive such replotting are assumed to be associated with the data set itself.

Corrections

The histograms must next be altered to compensate for a recording efficiency which is energy dependent on two counts. The "geometrical correction" recognizes that the event of an acceptable track passing out of the emulsion and consequently being rejected is more frequent for high energy recoil protons than for slow ones. This is corrected by the application of a calculated weighting function[8] dependent on the emulsion thickness and the maximum acceptable obliquity in the vertical plane.

The "cross-section correction" is a direct compensation for the energy dependence of the neutron-proton scattering cross section (on which neutron recording depends), and is accomplished by the use of a weighting function given by the reciprocal of the cross section as a function of energy. For the cross-section function, a smooth curve was drawn through various experimental determinations.[9] The total correction, the product of the two functions, is shown in Fig. 1 for the Eastman NTB emulsion (No. 347,126) used in the present experiments. In the region below 1 Mev the cross-section correction function drops very rapidly, so that normalization at 0 Mev is not practical. Both corrections were, therefore, normalized to unity at 2 Mev, where both functions were varying fairly slowly. The 2-Mev point happens also to represent the lower limit of reliable observation with the photographic and microscopic systems employed.

In practice, the correction function was applied to the histogram points before a curve was drawn. The apparent best fitting, smooth curve was then drawn through the corrected points, and the location of groups decided on the basis of it. The procedure outlined here was then followed to describe the groups quantitatively. The high energy side of the most energetic group was assumed to represent the true shape of its low energy side as well, the latter being distorted by the presence of the next less energetic group. The high side was, therefore, reflected about the estimated last peak, and subtracted from the curve. It was assumed that this revealed the true form of the high energy side of the next group, and the process was repeated. It is from the symmetrical group forms thus deduced from the observed curve that extrapolated ranges, widths, and intensities were taken. It was felt that this procedure was necessary, even when a complex spectrum afforded relatively little indi-

[9] R. Sherr, Phys. Rev. **68**, 240 (1945); E. O. Salant and N. F. Ramsey, Phys. Rev. **57**, 1075 (1940); M. Bunge, Nature **156**, 301 (1945); C. L. Bailey, W. E. Bennett, T. Bergstrahl, R. G. Nuckolls, H. T. Richards, and J. H. Williams, Phys. Rev. **70**, 583 (1946).

vidual group structure on which to base the deduced shapes.

The extrapolated ranges were corrected and reduced to mean ranges, following Bethe.[5] The corresponding mean energies were employed in the computation of Q-values.

4. THE ENERGY DISTRIBUTION CURVES

Al(αn)

A thick target of aluminum foil was bombarded with alpha-particles from the cyclotron, mean energy 7.64±0.14 Mev, the width (at half-value) 0.3 Mev. The distribution of 775 satisfactory tracks is displayed in Figs. 2 and 3. The data there represented were taken in two parts, so that the curve from 3.2 Mev up is based on about one third of the total number of tracks observed. This higher energy portion of the aluminum spectrum is shown in Fig. 3. The true yield of acceptable tracks per mm² per microampere-minute was distributed as follows: 2.0 to 4.0 Mev, 8.6×10^{-2}; 4.0 to 6.5 Mev, 4.3×10^{-4}; over 6.5 Mev, 4.3×10^{-5}; employing a 51-micron thick emulsion at grazing incidence, 19 cm from the target.

Two groups are indicated in Fig. 2; their poor definition is attributed to the use of a thick target (necessary for adequate yield) and the considerable energy spread of the alpha-particle beam. That they are separate groups, suggested by the curve form, is confirmed by their widths (0.6 Mev each) which individually are greater than that of the beam. The extrapolated ranges of these groups correspond to 3.58±0.05 and 2.63±0.07 Mev. They are attributed to the reaction (1) and give values $Q_1=-2.93\pm0.17$ and $Q_1'=-3.91\pm0.19$ Mev.

The rare tracks above 3.9 and extending as high as 10.7 Mev may well be caused by the reaction

$$Al^{27}+D^2=Si^{28}+n^1+Q_5, \qquad (5)$$

excited by the residual deuteron beam in the cyclotron. A maximum neutron energy of 11.7 Mev is expected for this reaction. Another possible origin of the occasional high energy tracks is the primary cosmic radiation. This hypothesis will be discussed at the end of the paper. In considering the possibility of two sources of the high energy particles, the marked decrease in yield which occurs around 6.5 Mev may be of interest. For, while cosmic radiation seems a reasonable cause for the rare tracks above 6.5 Mev, those from 4.0 to 6.5 Mev seem too abundant to be so explained.

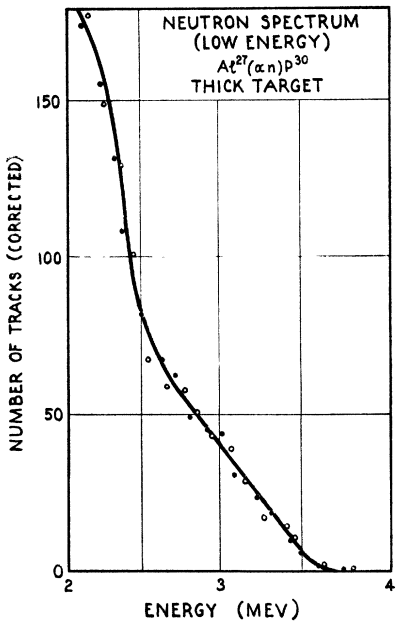

FIG. 2. Neutrons from Al²⁷+He⁴. 500 tracks, from 4.3 cm² of plate area. Ordinates corrected for geometrical and cross-section effects (correction factor plotted in Fig. 1). Each set of points represents number of tracks in 200-kev interval taken every 100 kev. The two point sets are displaced approximately 50 kev. Re abscissae, see text.

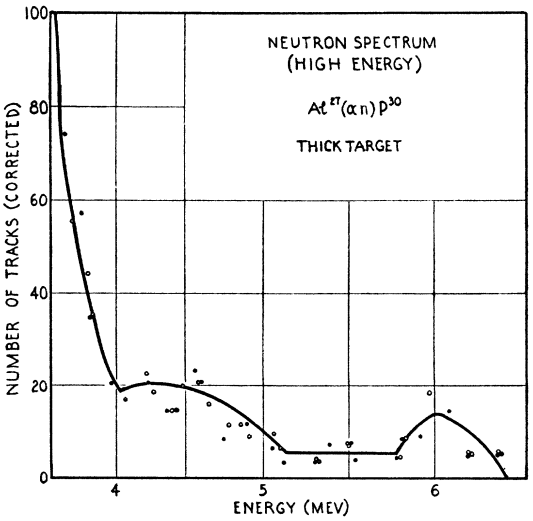

FIG. 3. Neutrons from Al²⁷+He⁴. 275 tracks from 85 cm² of plate area. Additional tracks (not plotted): 7.16–7.54–8.70–10.57–10.73 Mev. Otherwise as Fig. 2.

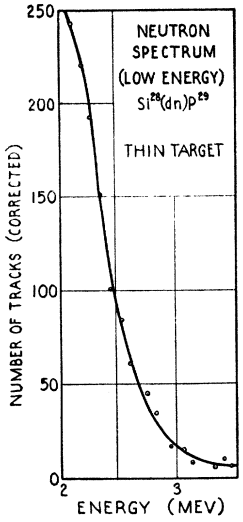

FIG. 4. Neutrons from Si(*dn*)P. 600 tracks, from 1.1 cm² of plate area. Ordinate is number of tracks in 200-kev interval taken every 100 kev, corrected (Fig. 1). This is group X.

Si(*dn*)

The silicon target used was a thin film of the pure element[10] (1 mg/cm², equivalent to 6 mm of air) deposited by evaporation on a thick gold foil. It was bombarded with deuterons of mean energy 3.72±0.07 Mev and width 0.17 Mev. Approximately 1500 tracks are represented in the distribution of Figs. 4 and 5. As with the aluminum spectrum, certain regions were emphasized, when the data were taken, to gain definition. The distribution of the 1500 tracks is therefore roughly as follows: 2.0 to 3.75 Mev, 45 percent; 3.75 to 4.65 Mev, 20 percent; above 4.65 Mev, 35 percent. The peak height of the most energetic group in Fig. 5 represents 1.53 $\times 10^{-4}$ acceptable tracks per mm² per microampere-minute of exposure, in a 51-micron thick emulsion at glancing incidence, 18 cm from the target.

This silicon spectrum is the composite of separate spectra from the reactions on the three constituent isotopes Si^{28}, Si^{29} and Si^{30} of abundances, respectively, 89.6, 6.2, and 4.2 percent. The groups which appear are listed in Table I.

5. RESULTS AND INTERPRETATION

Aluminum

The group from the ground-state transition in reaction (1) yielded the value $Q_1 = -2.93 \pm 0.17$ Mev. The observed threshold for (1), as indi-

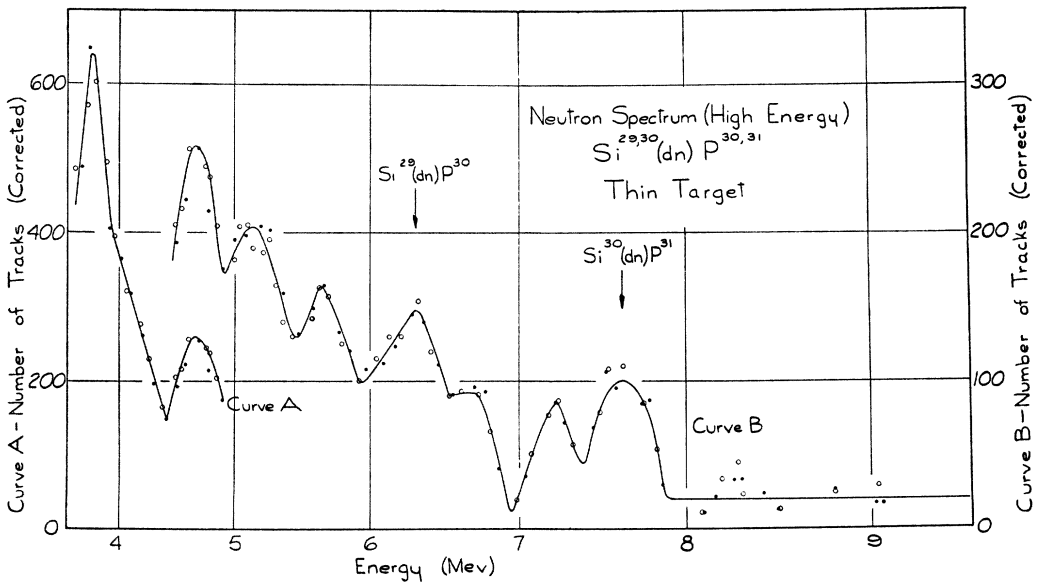

FIG. 5. Neutrons from Si(*dn*)P. 900 tracks, from 62 cm² of plate area. Additional tracks (not plotted): 9.92–10.38–10.46 Mev. Otherwise as Fig. 2. Groups are called I to IX, from right to left.

[10] Impurities not over a few thousandths of a percent. I am indebted to the Bell Telephone Laboratories for the pure silicon from which this target was prepared.

cated in the Introduction, is about 2.0 ± 0.2 cm alpha-particle range, corresponding to 3.4 ± 0.4 Mev in energy, and $Q_1=-2.9\pm0.3$ Mev; Bethe's prediction[5] is $Q_1=-3.3$ Mev.

The value of Q_1 here observed leads to the mass difference

$$P^{30}-Al^{27}=2.998\ 06\pm0.24\times10^{-3}\text{ mass units},$$

and, with Mattauch's listing[11] for aluminum, to

$$P^{30}=29.988\ 75\pm0.67\times10^{-3}\text{ mass units}.$$

This is consistent with 29.988 5 which was derived[11] from the beta-ray upper limit of P^{30}.

The lower energy group here observed in the aluminum spectrum, $Q_1'=-3.91\pm0.19$ Mev, corresponds to a transition to an excited level in P^{30}, 1.02 ± 0.12 Mev above ground.

Silicon 28

Group X of Table I may be identified immediately with the reaction (2) by virtue of its yield, Si^{28} being 89.6 percent abundant. The observed energy change, $Q_2=-0.80\pm0.10$ Mev, gives the mass difference

$$P^{29}-Si^{28}=1.006\ 64\pm0.14\times10^{-3}\text{ mass units}$$

and, with Mattauch's listing[11] for Si^{28},

$$P^{29}=28.993\ 87\pm0.59\times10^{-3}\text{ mass units}.$$

No comparison value for Q_2 has been located, but a P^{29} mass can be calculated[11] on the basis of the beta-spectrum of that nucleus.[12] It is $P^{29}=28.991\ 51$ mass units. The discrepancy between this and the above value is considerable, but the present identification of group X seems unambiguous.

Silicon 29

The group from the ground-state transition in reaction (3) may be located in terms of the mass of P^{30}, determined from the present investigation of reaction (1). The value thus predicted is $Q_3=3.30\pm1.23$ Mev, which indicates strongly that IV of Table I is the group arising from the ground-state transition in the reaction (3). Bethe's prediction[5] of 3.9 Mev may be compared.

[11] S. Flügge and J. Mattauch, Physik. Zeits. **42**, 1 (1941); also, J. Mattauch, *Nuclear Physics Tables* (Interscience Publishers, Inc., New York, 1946), Table IV.

[12] M. G. White, E. C. Creutz, L. A. Delsasso, and R. R. Wilson, Phys. Rev. **59**, 63 (1941).

TABLE I. Neutron groups in the composite spectrum Si(*dn*)P. Reliability is based on comparison of group elevation (peak over valley preceding) with the square root of the peak yield. *A*: elevation is greater than $N^{\frac{1}{2}}$, *B*+: elevation is approximately equal to $N^{\frac{1}{2}}$, *B*: elevation is less than $N^{\frac{1}{2}}$, *C*: no peak appears (group deduced from break in the slope of the curve).

Group	Extrapolated range (Mev)	Half-value width (Mev)	Relative intensity	Reliability	*Q* (Mev)
X	2.62 ± 0.02	0.64	~140.	*A*	-0.80 ± 0.10
IX	4.12 ± 0.06	0.38	5.5	*A*	0.71 ± 0.13
VIII	4.43 ± 0.04	0.28	2.5	*C*	1.03 ± 0.11
VII	4.92 ± 0.08	0.30	2.2	*A*	1.52 ± 0.15
VI	5.49 ± 0.23	0.54	1.8	*B*	2.11 ± 0.31
V	6.15 ± 0.09	0.50	1.6	*A*	2.78 ± 0.16
IV	6.76 ± 0.10	0.44	1.5	*A*	3.38 ± 0.17
III	6.93 ± 0.08	0.20	0.8	*B*	3.57 ± 0.15
II	7.47 ± 0.09	0.26	0.8	*B*+	4.12 ± 0.16
I	7.90 ± 0.06	0.36	1.0	*A*	4.56 ± 0.13

This Q_3 value provides a determination of the Si^{29} mass, thus:

$$P^{30}-Si^{29}=1.002\ 15\pm0.21\times10^{-3}\text{ mass units}$$

and, with the mass of P^{30} determined from the Al(αn) reaction,

$$Si^{29}=28.986\ 60\pm0.88\times10^{-3}\text{ mass units}.$$

The corresponding value listed[11] is 28.986 51. An internal consistency check is possible between reactions (1) and (3), in terms of the equation derived by eliminating the unknown P^{30} mass from the *Q*-value expressions, *viz.*,

$$Q_3-Q_1=Si^{29}-Al^{27}+D^2-He^4. \qquad (6)$$

The right-hand member of (6), dependent only on masses of stable nuclei, has the value 6.23 Mev, while the left-hand member, as observed here, is $+3.38-(-2.93)=6.31$ Mev, in good agreement.

Silicon 30

The remaining groups (I, II and III) of Table I are assigned to the remaining isotope, in reaction (4). The most energetic group (I) corresponds to $Q_4=4.56\pm0.13$ Mev, for which Bethe's prediction[5] is 4.3 Mev. This observation determines the mass difference

$$P^{31}-Si^{30}=1.000\ 88\pm0.18\times10^{-3}\text{ mass units}.$$

For this reaction, both involved nuclei are stable. The mass of P^{31} is better known than

TABLE II. Interpretation of the neutron groups in Table I. Means of identification are amplified in text, under "Results and Interpretation."

Means of identification	Group	Reaction	Final nucleus	Q (Mev)	Excitation (Mev)	Comparison excitation (Mev)	Comparison reference
Sole isotope	I	(4)	P^{31}_{gnd}	4.56±0.13	0.00		
Sole isotope	II	(4)	P^{31*}	4.12±0.16	0.44±0.29		
Sole isotope	III	(4)	P^{31**}	3.57±0.15	0.99±0.28	1.05	Haxel,† Bethe††
Q predicted	IV	(3)	P^{30}_{gnd}	3.38±0.17	0.00		Reaction (1)
Sole isotope, and level predicted	V	(4)	P^{31***}	2.78±0.16	1.78±0.29	1.7	Haxel,† Bethe††
Level predicted	VI	(3)	P^{30*}	2.11±0.31	1.27±0.48	1.02±0.12	Reaction (1)
Ambiguous	VII	(3), (4)	$P^{30,31}$	1.52±0.15			
Ambiguous	VIII	(3), (4)	$P^{30,31}$	1.03±0.11			
Ambiguous	IX	(3), (4)	$P^{30,31}$	0.71±0.13			
Abundance	X	(2)	P^{29}_{gnd}	−0.80±0.10	0.00		

† See reference 14.
†† See reference 5.

Si^{30}, however, so Mattauch's value[11] for the former is used, with the above mass difference, to find

$$Si^{30} = 29.983\ 53 \pm 0.45 \times 10^{-3} \text{ mass units.}$$

The corresponding listing[11] is $29.983\ 99 \pm 0.50 \times 10^{-3}$ units. An internal consistency checking equation may be derived by considering, in addition to (3) and (4), the activity (positron) of P^{30}, decaying into Si^{30}. The reported upper limit for the positron spectrum[13] is alternatively 3.0 or 3.5 Mev, corresponding to $Q_7 = 4.26 \pm 0.25$ Mev, if Q_7 is used to denote the energy release in the activity mentioned. The checking relation is

$$Q_3 + Q_4 = 2D^2 - 2n^1 + Si^{29} - P^{31} - Q_7. \qquad (7)$$

The right-hand member of (7), depending only on stable masses and Q_7 just mentioned, has the value 8.4±1.1 Mev. The left-hand member as here observed is $3.38 + 4.56 = 7.94 \pm 0.30$ Mev, in adequate agreement.

Energy Levels

No excited state transitions in reaction (2) were observed, because of its low Q-value. The remaining groups of Table I may to some extent be distributed between the remaining reactions (3) and (4), as in Table II. The identification of groups I, II, III, IV, and X has already been discussed. Group VI is associated with reaction (3) and the formation of P^{30} in its 1-Mev excited state, that state having been established in reaction (1). Then, since no lower level intervened in (1), it is assumed that the intervening group V is not associated with P^{30}, and, consequently, derives from reaction (4) and a third excitation level in P^{31}. This identification is confirmed by an independent observation of the same level by Haxel,[14] in studying the reaction

$$Si^{28} + He^4 = P^{31} + H^1 + Q_8. \qquad (8)$$

Groups VII, VIII, and IX remain ambiguous, identified either with reaction (3) or (4).

Intensity Ratios

The ratio of the yield from the ground-state transition in reaction (3) to that from the ground-state transition in (4) is given by the ratio of group intensities IV:I and is equal to 1.5. The ratio of the target isotope abundances (Si^{29}:Si^{30}) is 6.2:4.2 = 1.5. This indicates that the cross section for the ground-state transition in (3) and that in (4) are equal at the bombarding energy employed.

The yield ratio P^{29}_{gnd}:(mean of P^{30}_{gnd} and P^{31}_{gnd}) is given by the group intensities X:(mean of I and IV), and is equal to 110. The corresponding target isotope abundance ratio is 89.6:5.2, only 17. The cross section for the ground-state transition in reaction (2), therefore, seems to be greater than that for the same transition in (3) and (4) by a factor about 6.5.

In reaction (8), Haxel[14] found intensity ratios 1.0:1.8:2.4 for transitions to the ground, first excited, and second excited states of P^{31}, respec-

[13] G. T. Seaborg, Rev. Mod. Phys. 16, 4 (1944).

[14] O. Haxel, Physik. Zeits. 36, 804 (1935).

tively. The intensities of the corresponding neutron groups are 1.0:0.8:1.6 for I:III:V. However no group observed by Haxel corresponds to the present II. If the intensity of this group is added to that of III, the ratios are I:(II+III):V =1.0:1.6:1.6 and the remaining discrepancy, amounting to less than a factor 2, is in the third excited level transition. In any event, two different reactions—(4) and (8)—are involved, and a selection rule may be indicated.

A similar comparison is possible for yields from the ground and first excited state transitions to P^{30} as revealed, on the one hand, in reaction (1), on the other, in (3). For (3), the ratio is given by ground:first excited = IV:VI = 1.5:1.8 =1.0:1.2. For reaction (1), the corresponding ratio is not definitely determinate from Fig. 2, but is certainly greater than 2.8, in distinct disagreement with 1.2, above. Again, a selection rule may be involved.

High Energy Background Tracks

The silicon spectrum was terminated with group I on the basis of yield, for a distinct reduction in intensity characterizes the tracks following. Additional data taken in the range above 8 Mev show no organization into groups, but only a scattered background extending as far as 10.5 Mev. It is unlikely that these tracks derive from a reaction on the target, since the latter is believed to have been very pure and any appreciable contamination of the deuteron beam is very unlikely. It is believed that the high energy background observed in both the silicon and aluminum reactions is attributable to cosmic rays. The qualitative features supporting this idea follow.

The background seems independent of the exposure and of the reaction recorded, appearing on all plates. For example, the background intensity in the presence of reaction (1) was of order 1 track per plate, the cyclotron exposure having been 12.5 microampere-minutes. The background intensity accompanying the silicon reactions was only of order 4 per plate, however, though the exposure in that case was 330 microampere-minutes.

Observations[15] have shown approximately 0.1 track per cm^2 per day accumulating in photographic emulsions due to cosmic rays, corresponding to 1.5 tracks per plate per day, for 1×3 inch plates. The present data show roughly 3 tracks per plate after five months, entirely consistent (300 per plate) when corrected for the angular discrimination practiced in recording track data. Further, these 300 (deduced) single tracks per plate are accompanied by between 0.1 and 1.0 cosmic-ray "star" per plate, a frequency which is consistent with the expectation[15] of roughly 200 single tracks per star.

Finally, the cosmic-ray track distribution previously recorded[15] has its peak at about 13 Mev and a width of 8 Mev (at half-intensity), which distribution is expected to be degraded in energy at sea level. It has, therefore, the right location to account for the background observed around 10 Mev without providing an equal or greater disturbance at the lower energies.

The assistance of Professor R. F. Humphreys throughout this project is gratefully acknowledged.

[15] Edited by W. Heisenberg, *Cosmic Radiation* (Dover Publications, New York, 1946), Chapter 13.